



## Extensive analysis of pollutant interactions: Identification of deleterious synergistic effects at environmentally relevant dose levels using *Drosophila* and mammalian cells

Francisco Alejandro Lagunas-Rangel<sup>a,b,\*</sup>, Martin Åberg<sup>c</sup>, Sifang Liao<sup>a</sup>, Felipe Espinelli-Amorim<sup>a</sup>, Rajanidevi Tummaramatti-Hanumant<sup>a</sup>, Ludmila Jackeoviča<sup>b</sup>, Monta Briviba<sup>d</sup>, Wen Liu<sup>a</sup>, Robert Fredriksson<sup>e</sup>, Ahmed M. Alsehli<sup>f</sup>, Ola Spjuth<sup>f</sup>, Janis Klovins<sup>g</sup>, Maija Dambrova<sup>b</sup>, Błażej Kudłak<sup>h</sup>, Claes Andersson<sup>c</sup>, Helgi B. Schiöth<sup>a,b,\*\*</sup>

<sup>a</sup> Department of Surgical Sciences, Functional Pharmacology and Neuroscience, Uppsala University, Uppsala, Sweden

<sup>b</sup> Laboratory of Pharmaceutical Pharmacology, Latvian Institute of Organic Synthesis, Riga, Latvia

<sup>c</sup> Department of Medical Sciences, Uppsala University, Uppsala, Sweden

<sup>d</sup> Translational Omics Group, Latvian Biomedical Research and Study Centre, Riga, Latvia

<sup>e</sup> Department of Pharmaceutical Biosciences, Uppsala University, Uppsala, Sweden

<sup>f</sup> Department of Physiology, Faculty of Medicine, King Abdulaziz University, Jeddah, Kingdom of Saudi Arabia

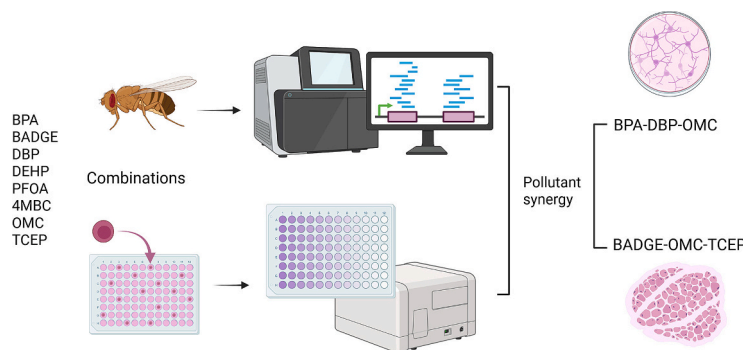
<sup>g</sup> Genome Centre, Latvian Biomedical Research and Study Centre, Riga, Latvia

<sup>h</sup> Department of Analytical Chemistry, Faculty of Chemistry, Gdańsk University of Technology, Gdańsk, Poland

### HIGHLIGHTS

- There are more synergistic interactions between pollutants than previously thought.
- BPA-DBP-OMC mixture has detrimental effects on neuronal differentiation.
- BADGE-OMC-TCEP mixture has negative impact on muscle differentiation.

### GRAPHICAL ABSTRACT



### ARTICLE INFO

Editor: Lidia Minguez Alarcon

#### Keywords:

Pollutant mixtures

### ABSTRACT

Environmental pollutants are commonly present in low concentrations, often as complex mixtures that can lead to various interaction phenomena, including synergism, antagonism, or additive effects. These interactions can alter the overall toxicity or biological impact of the mixture when compared to the effects of individual pollutants. While regulatory agencies typically assess the safety of individual pollutants, the cumulative and

\* Corresponding author at: Laboratory of Pharmaceutical Pharmacology, Latvian Institute of Organic Synthesis, Aizkraukles 21, LV-1006 Riga, Latvia.

\*\* Correspondence to: H.B. Schiöth, Department of Surgical Sciences, Functional Pharmacology and Neuroscience, Uppsala University, BMC Box 593, Husargatan 3, 751 24 Uppsala, Sweden.

E-mail addresses: [francisco.lagunas@farm.osi.lv](mailto:francisco.lagunas@farm.osi.lv) (F.A. Lagunas-Rangel), [helgi.schioth@uu.se](mailto:helgi.schioth@uu.se) (H.B. Schiöth).

<https://doi.org/10.1016/j.scitotenv.2025.179848>

Received 8 April 2025; Received in revised form 3 June 2025; Accepted 4 June 2025

Available online 25 June 2025

0048-9697/© 2025 The Author(s). Published by Elsevier B.V. This is an open access article under the CC BY license (<http://creativecommons.org/licenses/by/4.0/>).

Bisphenol a  
Phthalates  
Endocrine disruptors  
RNA-seq

interactive effects of pollutant mixtures are less well understood. This study aims to address this gap by evaluating the interactions of eight common pollutants (BPA, BADGE, DBP, DEHP, PFOA, 4MBC, OMC, TCEP) at their no observed effect level (NOEL) concentrations. The study specifically focuses on identifying potential synergistic effects on cell viability, transcriptomic changes, and phenotypic outcomes in two biological models: *Drosophila* and mammalian cell lines. Nearly 400 combinations of pollutants were tested, and their effects were compared to those of individual pollutants and appropriate controls. The results highlighted significant findings, including detrimental effects of the BPA-DBP-OMC mixture on neuronal differentiation and the BADGE-OMC-TCEP mixture's negative impact on muscle differentiation on *Drosophila* and mammalian cell lines. Cytotoxic synergy effects were also found between bisphenol derivatives and phthalates. These findings emphasize the need to consider the risks associated with pollutant mixtures.

## 1. Introduction

Environmental pollutants are substances that have been released into ecosystems and pose significant health risks to living organisms exposed to them. These pollutants are widespread and often resist degradation over long periods resulting in daily exposure to humans (Lagunas-Rangel et al., 2022a). It is estimated that these compounds contribute to 9 million deaths per year, representing 16 % of all deaths worldwide, three-fold more deaths than from acquired immunodeficiency syndrome, tuberculosis and malaria combined. From an economic perspective, pollution led to global losses amounting to US\$4.6 trillion in 2015, equivalent to 6.2 % of the world's economic output (Landrigan et al., 2018). Despite all these important implications, pollution research has often been largely ignored by international development and global health agendas. The health risks posed by environmental pollutants continue to be underrepresented in global burden of disease assessments, leading to an underestimation of their true effects on public health (Fuller et al., 2022). Moreover, the combined effects of exposure to multiple pollutants are often overlooked in regulatory practices (Bopp et al., 2018).

Most environmental pollutants are present in low concentrations, often below toxicity thresholds, and usually exist as complex mixtures (Goodson et al., 2015). These mixtures can be the result of preformed cocktails emitted by a single source or of different pollutants released from various sources that are then combined in the same environmental space (Lagunas-Rangel et al., 2022b). Each pollutant in the mixture can affect the other components in a variety of ways, resulting in complex interaction phenomena. These interactions can enhance the effects of pollutants, creating a synergistic response, or reduce their effects through antagonism. In some cases, the effects of pollutants may simply add up, resulting in additive interactions (Geary, 2013; Niu et al., 2019). In this way, these interactions can alter toxicity or biological impact of the mixture as a whole, often resulting in outcomes that differ from those of the individual pollutants separately (Jatkowska et al., 2021; Rafeletou et al., 2024).

There is growing concern that mixtures of pollutants, even in concentrations considered innocuous individually, can produce harmful synergistic effects. This raises questions about whether compliance with individual environmental quality standards is sufficient to protect against the toxic impacts of these mixtures (Brack, 2015; Cedergreen, 2014). Addressing this issue calls for a more comprehensive approach to assessing and managing the risks associated with exposure to pollutant mixtures. It also highlights the critical need for further research into the interactions between an increasingly wide range of pollutants and development of the current methods and approaches. More data and better approaches are essential to understand their combined effects and to develop effective strategies to minimize potential health and environmental risks (Cedergreen, 2014; Fuller et al., 2022).

Pollutants can interact in various ways, creating synergies through different mechanisms. For example, two compounds could influence the same or different steps within the same biochemical pathway (Cedergreen, 2014). The presence of one pollutant could also affect the other by enhancing or inhibiting its action, or it could alter the amount or dose of the other pollutant available to produce biological effects

(Lagunas-Rangel et al., 2022b). A previously published review by our team provides an in-depth analysis of the underlying mechanisms, highlighting reactive oxygen species (ROS) overproduction and aryl hydrocarbon receptor (AhR) activation as key factors driving these synergies and their deleterious effects (Lagunas-Rangel et al., 2022b). Other mechanisms involve alterations in growth factor and hormone signaling pathways, mitochondrial dysfunction, and imbalances in proapoptotic and antiapoptotic signaling, among other cellular processes (Boobis et al., 2011; Kudlak et al., 2022; Mauderly and Samet, 2009).

With all this in mind, the aim of this study was to evaluate the interactions of eight common pollutants (bisphenol A [BPA], bisphenol A diglycidyl ether [BADGE], dibutyl phthalate [DBP], di(2-ethylhexyl) phthalate [DEHP], perfluorooctanoic acid [PFOA], tris(2-chloroethyl) phosphate [TCEP], 4-methylbenzylidene camphor [4-MBC] and octyl-methoxycinnamate [OMC]) at their no observed effect level (NOEL) concentrations and to identify possible synergistic effects on cell viability, transcriptomic changes and phenotypic outcomes in two biological models, *Drosophila* and mammalian cell lines. The main toxicological mechanisms of these pollutants primarily involve endocrine disruption, oxidative stress, and interference with cellular signaling. BPA and BADGE are thought to act as xenoestrogens, binding to estrogen receptors and disrupting hormonal balance (Poole et al., 2004; vom Saal et al., 2012). DBP and DEHP are suggested to impair reproductive development by antagonizing androgen receptors and altering steroidogenesis, while also generating ROS that lead to oxidative stress (Heudorf et al., 2007). PFOA is linked to disruption of lipid metabolism and immune function via activation of peroxisome proliferator-activated receptors (PPARs) (Heudorf et al., 2007). TCEP is a neurotoxicant that inhibits acetylcholinesterase and induces oxidative stress and apoptosis (Li et al., 2019). 4-MBC and OMC are UV filters with estrogenic activity that interfere with endocrine signaling and may alter reproductive and thyroid hormone pathways (Rafeletou et al., 2024). Three hundred and ninety-six pollutant mixtures were tested and compared to the effects of individual pollutants and appropriate controls. Through this extensive analysis, we identified that a mixture of BPA-DBP-OMC has detrimental effects on neuronal differentiation, while a mixture of BADGE-OMC-TCEP negatively affects muscle differentiation. These findings highlight the potential risks associated with mixtures of contaminants, even at concentrations considered individually safe as well as providing foundation for further methodological development to test mixtures in large scale.

## 2. Materials and methods

### 2.1. Pollutants

Stock solutions of the following pollutants were prepared: BPA (Sigma-Aldrich, 133,027), BADGE (Sigma-Aldrich, D3415), DBP (Sigma-Aldrich, 524,980), DEHP (Sigma-Aldrich, 36,735), PFOA (Sigma-Aldrich, 171,468), TCEP (Sigma-Aldrich, C4706), 4-MBC (Sigma-Aldrich, 78,848) and OMC (Sigma-Aldrich, 78,848). The measured amounts of each compound were accurately weighed and dissolved in dimethyl sulfoxide (DMSO, Invitrogen, D12345) or pure

ethanol (Sigma, 1.00983) to prepare stock solutions with a final concentration of 10 mM. Dilutions were prepared from these stock solutions to achieve the particular concentrations desired for each study condition. DMSO was used as the solvent for experiments involving cell cultures, while ethanol was employed as the solvent for treatments in *Drosophila* models.

## 2.2. Cell lines and culture conditions

The cell lines used in this study were obtained from the German Collection of Microorganisms and Cell Cultures GmbH (DSMZ) and the American Type Culture Collection (ATCC). REH cells (ATCC-CRL-8286) were cultured in RPMI 1640 medium (Sigma R0883) supplemented with 10 % heat-inactivated fetal bovine serum (HI-FBS, Sigma F9665) and 2 % penicillin-streptomycin (Sigma, P0781) and L-Glutamine (Sigma, G7513) solution. C2C12 cells (ACC 565) were grown in DMEM medium with GlutaMAX Supplement (Gibco, 10566016), also supplemented with 10 % FBS (Gibco, A3160502) and 1 % penicillin-streptomycin solution (Gibco, 15140130). NTERA-2 cl.D1 cells (CRL-1973) were maintained in DMEM medium (ATCC, 30–2002) supplemented with 10 % FBS (ATCC, 30–2020) and 1 % penicillin-streptomycin solution (Gibco, 15140130). All cell lines were cultured in a humidified incubator at 37 °C with 5 % CO<sub>2</sub>.

## 2.3. Cell viability assays

A factorial model was designed to evaluate the combinations of pollutants, taking into account six concentration levels for each pollutant: 1 nM, 10 nM, 100 nM, 1 μM, 10 μM, and 100 μM. At least three independent biological replicates were performed for each group. Monocultures were established by seeding REH cells at a density of 7500 cells per 50 μL per well in a 384-well Corning plates (Thermo Fisher Scientific, 3764) using a Biomek 4000 (Beckman Coulter, Brea, CA, USA). After a 24-h pre-culture period, according to a plate layout, the pollutants and vehicle were loaded using acoustic dispensing with the Echo Liquid Handler 550 (Beckman Coulter). The final vehicle concentration varied as a function of pollutant dilution: 1 % for 100 μM, 0.1 % for 10 μM, 0.01 % for 1 μM, 0.001 % for 100 nM, 0.0001 % for 10 nM, and 0.00001 % for 1 nM. Appropriate vehicle controls were included for each concentration in each experiment, and no significant effects on cell viability were observed (data not shown). The treated plates were placed in an incubator during the 72-h incubation (37 °C, 95 % humidity with 5 % CO<sub>2</sub>). After incubation the plates were analyzed using the fluorometric microculture cytotoxicity assay (FMCA) to measure the cytotoxic effects of the pollutants (Lindhagen et al., 2008). The method utilizes the conversion of fluorescein diacetate (FDA) to fluorescein via esterase in intact plasma membranes of viable cells and this signal can be measured using a fluorescence reader (Clariostar, BMG Labtech, Ortenberg, Germany) (Blom et al., 2016). The viability was quantified as Survival Index (SI) =  $(f_{\text{Treatment}} - f_{\text{Blank}}) / (f_{\text{Control}} - f_{\text{Blank}})$  where  $f_i$  denotes the fluorescent signal in treated cells, untreated cells and blank wells respectively. The type of interaction between pollutants was determined based on the Bliss independence model (Goldoni and Johansson, 2007). The Bliss score was calculated using the formula:  $B = 100 \times (SI_1 \times SI_2 - SI_{1,2})$  where  $SI_1$  and  $SI_2$  corresponds to the SI for compound 1 and 2 individually and  $SI_{1,2}$  to the SI of the combination. A positive Bliss score indicates that the viability of the combination is lower than expected based on the individual pollutant treatments and the assumption of independent effects, suggesting a synergistic effect in reducing cell viability. Conversely, a negative Bliss score indicates that the viability of the combination is higher than expected based on the individual pollutant treatments and the assumption of independent effects, indicating an antagonistic effect favoring cell proliferation.

## 2.4. Fly strains and husbandry

Wild-type *Drosophila* fly lines, Canton-S and Oregon-R-C, were obtained from the Bloomington Stock Center (Bloomington, Indiana, USA) and crossed to establish the laboratory wild-type CSORC strain. Flies were reared on Jazz-Mix *Drosophila* food (Thermo-Fisher Scientific, AS153) supplemented with 1.5 % yeast extract (Apex Bio Research Products, 20–254), 0.3 % propionic acid (Sigma-Aldrich, 402,907), and 0.05 % tegosept (Apex Bio Research Products, 20–258). Cultures were maintained at 25 °C and 60 % relative humidity under a 12-h light/dark cycle, unless stated otherwise.

## 2.5. Fly feeding with pollutants

A simplified factorial model was designed to analyze the combined effects of three pollutants, using the corresponding NOEL concentrations of each pollutant as the baseline for the evaluation (Table 1). Male *Drosophila* flies were selected because they exhibit more consistent hormonal profiles and predictable social behavior under controlled conditions compared to female flies, which improves the reliability of the data (Brand et al., 2024). Ethanol (70 %) served as a solvent to dissolve pollutants, and the prepared solutions were thoroughly mixed with Jazz-Mix *Drosophila* food in glass bottles. To maintain consistency, an equivalent volume of ethanol was added to the control food mixture. The final ethanol concentration in the fly food was 0.02 %, achieved by adding 10 μL of either 70 % ethanol or pollutant stock solution or mixture (dissolved in 70 % ethanol) to 50 mL of fly food. Parental CSORC flies (F<sub>0</sub>) were placed in bottles containing control or pollutant-loaden food and allowed to lay eggs for 24 h, after which the adults were removed. The progeny (generation F<sub>1</sub>) was used for subsequent experiments. On the twelfth day after egg-laying, only male progeny was collected and maintained on food containing the same concentration of pollutant used during the egg-laying period. Male flies were chosen exclusively to eliminate variability arising from the different nutritional requirements of mated and unmated female flies.

## 2.6. Fly RNA sequencing and analysis

Seven-day-old male flies, previously fed with control or pollutant-containing food, were collected and preserved using RNA Later (Thermo-Fisher, AM7021). Sample processing and next-generation sequencing (NGS) were conducted at the Latvian Biomedical Research and Study Centre. Total RNA was extracted from flies using the AllPrep DNA/RNA Mini Kit (QIAGEN, Germany) following the manufacturer's instructions. Homogenization was performed with the FastPrep-24 instrument. RNA concentration and purity were assessed using a Qubit Fluorometer (ThermoFisher Scientific, USA), while integrity was determined via RNA Integrity Number (RIN) analysis on an Agilent 2100 Bioanalyzer (Agilent, USA). Ribosomal RNA depletion was carried out on 200 ng of total RNA using the MGIEasy rRNA Depletion Kit (MGI Tech Co. Ltd., China), and complementary DNA (cDNA) libraries were prepared with the MGIEasy RNA Directional Library Prep Set (MGI Tech Co. Ltd., China). NGS was performed on the DNBSEQ-G400RS platform

**Table 1**  
Pollutants studied and their NOEL concentrations.

Pollutant	Abbreviation	Description	[NOEL]*
Bisphenol A	BPA	Plasticizer	3 nM
Bisphenol A diglycidyl ether	BADGE	Plasticizer	1 μM
Dibutyl phthalate	DBP	Plasticizer	15 nM
Di(2-ethylhexyl) phthalate	DEHP	Plasticizer	20 μM
Perfluorooctanoic acid	PFOA	Surfactant	10 μM
4-methylbenzylidene camphor	4MBC	UV filter	1 μM
Octylmethoxycinnamate	OMC	UV filter	1 μM
Tris(2-chloroethyl) phosphate	TCEP	Flame retardant	1 μM

\* Source: European Chemicals Agency (<https://echa.europa.eu>).

(MGI Tech Co. Ltd., China) using the DNBSEQ-G400RS High-Throughput Sequencing Set (PE 150) (MGI Tech Co. Ltd., Wuhan, China), generating 150 bp paired-end reads. The study included the following experimental groups: control ( $n = 3$ ), individual pollutants at their NOAEL concentrations ( $n = 3$  per pollutant, 8 pollutants), and mixtures of pollutants ( $n = 3$  per mixture, 40 ternary mixtures). All RNA-seq FASTQ files obtained were paired-end. The quality of raw reads was assessed using the FastQC toolkit (Wingett and Andrews, 2018), and low-quality reads and adapter sequences were trimmed with Trimmomatic (Bolger et al., 2014). Processed reads were aligned to the release 6 plus ISO1 MT/dm6 *Drosophila* reference genome using HISAT2 (Kim et al., 2019). Gene expression was quantified with featureCounts (Liao et al., 2014), and poorly expressed genes with fewer than one count per million reads (1 CPM) in at least two samples were excluded from further analysis. Differential gene expression results were visualized using volcano plots. Raw counts were normalized, and differential expression analysis was conducted using the Limma package (Ritchie et al., 2015). Genes with a  $\log_2$  fold change ( $\log_2fc$ )  $> 1.0$  and a  $p$  adj-value  $< 0.01$  were classified as up-regulated, whereas those with  $\log_2fc < -1.0$  and a  $p$  adj-value  $< 0.01$  were classified as down-regulated. For each combination of pollutants studied, five volcano plots were generated to assess changes in gene expression. The first three plots compared each individual pollutant (A, B, and C) to the control group. The fourth plot analyzed the effects of the combined pollutant mixture relative to the control. Lastly, the fifth plot was specifically designed to identify potential synergistic effects within the mixture (Supplementary file 1). Gene ontology (GO) enrichment analysis was performed on all differentially expressed genes using the gProfiler server (Kolberg et al., 2023). Synergistic effects were calculated using the formula: (Pollutant Mixture vs. Control) - (Pollutant A vs. Control) - (Pollutant B vs. Control) - (Pollutant C vs. Control).

## 2.7. Locomotion and sleep/activity behavior

Male flies 6–7 days old were used for locomotor activity assays and sleep analysis. Locomotor activity was monitored using the *Drosophila* Activity Monitor System (DAMS) system (Trikinetics, Waltham, MA) over a 4-day period on a 12 h light/12 h dark (12 L: 12 D) cycle at 25 °C and 60 % humidity. Total activity counts and sleep duration were analyzed using a MATLAB toolkit (MathWorks, Natick, MA). More details about the behavioural work in flies are found here (Liao et al., 2024; Liu et al., 2021; Williams et al., 2020).

## 2.8. Differentiation protocols

Since RNA sequencing in *Drosophila* suggested impairments in neuronal and muscle differentiation, we investigated these processes in mammalian cell lines capable of undergoing differentiation. REH cells are lymphoblasts and do not possess the ability to differentiate into neuronal or muscle lineages. To this end, we used two models: NTERA-2 cl.D1, a human pluripotent embryonal carcinoma cell line that differentiates into neuronal lineages in response to retinoic acid; and C2C12, a mouse myoblast cell line that readily differentiates into contractile myotubes expressing characteristic muscle proteins.

NTERA-2 cl.D1 cells were exposed for one week to OMC (1  $\mu$ M), DBP (15 nM), BPA (3 nM), or their combination, while C2C12 cells were treated with TCEP (10 nM), OMC (1  $\mu$ M), BADGE (1  $\mu$ M), or their combination under the same conditions. In both cases, cell viability was not significantly affected by either the individual compounds or their mixtures, indicating that the selected concentrations were non-cytotoxic and the experiments could proceed as planned (data not shown).

For differentiation of C2C12 cells, cells were seeded in a 6-well Nunclon Vita plate (Thermo Fisher, 145,380). The next day, once the cells reached 60–80 % confluence, the growth medium (DMEM with 10 % FBS) was replaced with differentiation medium (DMEM supplemented with 2 % horse serum) with or without pollutants. Cells were

maintained in differentiation medium with individual pollutants or in combination (BADGE-OMC-TCEP) for 12 days, with medium changes every other day. A control group of cells was treated with the differentiation medium containing the vehicle only, without any pollutant, to maintain experimental consistency. After 12 days, differentiated cells were harvested by scraping with a scalpel in RIPA lysis buffer (Thermo-Fisher, R0278) containing protease inhibitor cocktail (Roche, 11,836,170,001) for protein extraction. Three replicates were performed for each experimental condition.

To induce differentiation of NTERA-2 cl.D1 cells, cells were seeded in a 6-well Nunclon Vita plate (Thermo Fisher, 145,380). The next day, when the cells reached 60–80 % confluence, differentiation was initiated by adding 10  $\mu$ M retinoic acid (Sigma-Aldrich, R2625) to the culture medium. The retinoic acid treatment was renewed twice a week, and the differentiation process was maintained for 4 weeks. Also, during this period, cells were exposed to individual pollutants or in combination (BPA-DBP-OMC), depending on the experimental set-up. A control group of cells was treated with the differentiation medium containing the vehicle only, without any pollutant, to maintain experimental consistency. At the end of the experiment, cells were harvested by scraping with a scalpel in RIPA lysis buffer (Thermo-Fisher, R0278) containing protease inhibitor cocktail (Roche, 11,836,170,001) for protein extraction. Three replicates were performed for each experimental condition.

## 2.9. Western blots

The protein content in the extracts was quantified using the Lowry method. For all samples, 20  $\mu$ g of total protein extract was separated using a Mini-PROTEAN TGX gel (Bio-Rad, 4,561,094) and transferred to a PVDF membrane (Invitrogen, IB24001) using the iBlot 2 system (Invitrogen). The membrane was blocked with 5 % nonfat milk in PBS for 1 h at room temperature, after which it was incubated overnight at 4 °C with primary antibodies at concentrations recommended by the supplier. After three washes with PBST buffer (PBS with 0.1 % Tween-20), the membrane was incubated with a goat anti-rabbit secondary antibody (Invitrogen, 31,460) for 1 h at room temperature and washed again. Actin (BD Biosciences, 612,656) served as a loading control, processed under identical conditions. The primary antibodies used were PAX7 (Invitrogen, PA-114), myosin heavy chain (Invitrogen, MA5-35613), desmin (Proteintech, 16,520-1-AP),  $\beta$ III tubulin (Invitrogen, PA5-80198), MAP2 (Invitrogen, PA5-17646), and nestin (Proteintech, 19,483-1-AP). The membranes were developed using the chemiluminescent substrate SuperSignal West Pico PLUS (Thermo Fisher, 1,863,096). Protein bands were then visualized using the Azure c400 gel imaging system (Azure Biosystems). Three independent replicates of each differentiation protocol were performed. Protein band intensities were quantified using Image Studio Lite software (LI-COR Biosciences). Expression levels were calculated as the ratio of each marker to actin (loading control) and normalized to the reference condition, defined as the sample not exposed to differentiation factors or pollutants (band 1).

## 2.10. Statistical analysis

Statistical analysis and graph generation were performed with GraphPad Prism version 9 (La Jolla, CA, USA). Parametric data are presented as mean  $\pm$  SD, whereas nonparametric data are expressed as median  $\pm$  SEM. Normality of the data was assessed by the Shapiro-Wilk test. For comparisons between groups, one-way analysis of variance (ANOVA) followed by Tukey's or Dunnett's multiple comparisons test was used for parametric data. For nonparametric data, the Kruskal-Wallis test with multiple comparisons was applied. Data with a  $p$  value  $\leq 0.05$  were considered significant.

**Table 2**  
**Matrix of analyzed pollutant mixtures and their corresponding Bliss scores.** The color intensity represents the type and degree of interaction: darker red indicates stronger synergy in promoting cell death, while lighter pink represents minimal synergy. Gray squares denote additive interactions within the pollutant combinations. Blue squares indicate synergy for cell growth. Empty cells represent combinations that were not analyzed. Cell viability measurements were referenced against untreated controls, vehicle-treated cells, and cells exposed to individual pollutants.

		10 nM						
		BPA	BADGE	DBP	DEHP	PFOA	OMC	4MBC
1 nM	BPA		22.1	25.1	11.3	11.3	12.0	12.5
	BADGE	20.3		23.8	20.2	22.2	22.1	24.9
	DBP	20.2	28.7		13.5	22.0	21.7	24.0
	DEHP	21.0	22.7	29.3		18.0	19.3	18.7
	PFOA	20.3	23.3	21.6	20.1		15.0	12.4
	OMC	21.2	19.6	16.7	18.2	5.3		11.1
	4MBC	28.5	22.7	15.7	22.3	12.7	16.5	
		100 nM						
		BPA	BADGE	DBP	DEHP	PFOA	OMC	4MBC
1 nM	BPA		-8.2	27.8	-3.7	4.7	11.1	0.0
	BADGE	14.6		4.4	5.6	10.1	20.7	7.0
	DBP	15.0	9.6		-5.6	5.4	19.5	3.8
	DEHP	22.4	11.9	2.9		9.5	17.5	1.8
	PFOA	27.7	16.5	-1.3	-4.7		21.0	1.5
	OMC	20.8	17.1	-2.2	-8.9	10.1		-4.9
	4MBC	21.2	13.3	-0.2	-1.4	9.7	20.5	
		1 μM						
		BPA	BADGE	DBP	DEHP	PFOA	OMC	4MBC
1 nM	BPA		-0.1	24.0	18.5	13.5	4.0	15.7
	BADGE	22.1		25.7	17.0	19.2	11.2	20.1
	DBP	20.3	33.8		16.6	26.2	11.6	23.2
	DEHP	29.5	20.2	15.5		11.1	2.6	12.3
	PFOA	26.5	21.2	13.5	22.4		7.2	14.1
	OMC	25.8	23.1	15.2	16.8	16.6		8.8
	4MBC	29.9	18.3	13.3	20.2	15.9	7.5	
		10 μM						
		BPA	BADGE	DBP	DEHP	PFOA	OMC	4MBC
1 nM	BPA		-1.1	2.7	-2.1	5.2	5.4	-1.2
	BADGE	4.4		5.9	7.4	10.8	1.4	0.2
	DBP	4.9	1.3		0.3	12.4	6.9	-0.3
	DEHP	10.0	3.1	1.5		7.1	5.8	0.2
	PFOA	6.8	11.4	5.0	4.3		6.1	0.4
	OMC	12.7	10.4	7.5	-0.3	11.4		2.4
	4MBC	2.6	7.9	1.9	0.3	7.9	8.1	
		100 nM						
		BPA	BADGE	DBP	DEHP	PFOA	OMC	4MBC
1 nM	BPA		0.0	7.4	10.0	10.9	6.1	1.2
	BADGE	13.1		14.5	14.7	21.7	8.8	3.1
	DBP	8.8	0.0		8.9	18.2	7.8	0.2
	DEHP	8.1	-0.1	8.2		14.8	9.8	2.8
	PFOA	9.2	0.0	10.3	14.8		7.7	2.7
	OMC	6.9	-0.1	5.7	14.3	5.2		10.5
	4MBC	6.4	0.0	6.4	11.5	7.0	10.3	
		1 μM						
		BPA	BADGE	DBP	DEHP	PFOA	OMC	4MBC
1 nM	BPA							
	BADGE	6.5						
	DBP	-1.5	1.5					
	DEHP	-8.2	6.8	7.3				
	PFOA	-0.4	10.2	8.1	3.8			
	OMC	-1.0	8.8	5.6	-1.3	0.8		
	4MBC	-8.4	8.9	4.3	8.2	7.0	-1.7	
		10 nM						
		BPA	BADGE	DBP	DEHP	PFOA	OMC	4MBC
10 nM	BPA							
	BADGE	15.1						
	DBP	11.5	12.7					
	DEHP	11.4	7.3	15.0				
	PFOA	7.1	11.0	12.8	3.6			
	OMC	10.4	12.3	7.6	2.1	3.9		
	4MBC	9.5	9.4	8.5	-0.6	-5.4	-4.2	
		100 nM						
		BPA	BADGE	DBP	DEHP	PFOA	OMC	4MBC
100 nM	BPA							
	BADGE	23.6						
	DBP	25.5	28.7					
	DEHP	21.8	29.6	20.9				
	PFOA	19.6	24.2	19.0	20.1			
	OMC	25.8	21.1	19.8	25.8	0.0		
	4MBC	12.7	20.5	25.8	6.0	26.1	26.7	
		1 μM						
		BPA	BADGE	DBP	DEHP	PFOA	OMC	4MBC
1 μM	BPA							
	BADGE	20.5						
	DBP	20.0	15.3					
	DEHP	13.3	23.4	23.0				
	PFOA	13.6	18.7	20.8	14.5			
	OMC	16.3	16.3	12.7	10.9	10.4		
	4MBC	10.0	22.4	13.5	6.7	15.2	8.4	
		10 μM						
		BPA	BADGE	DBP	DEHP	PFOA	OMC	4MBC
10 μM	BPA							
	BADGE	15.5						
	DBP	8.2	8.3					
	DEHP	12.9	4.2	4.2				
	PFOA	12.9	13.9	4.6	0.7			
	OMC	14.3	8.7	5.2	3.0	7.2		
	4MBC	7.2	9.4	3.4	-0.1	-4.2	-5.5	
		100 μM						
		BPA	BADGE	DBP	DEHP	PFOA	OMC	4MBC
100 μM	BPA							
	BADGE	-0.1						
	DBP	20.4	0.0					
	DEHP	15.3	0.0	5.5				
	PFOA	7.0	0.0	8.0	8.1			
	OMC	17.4	0.0	5.9	-6.4	18.8		
	4MBC	8.6	-0.1	13.3	-2.7	15.7	9.5	

### 3. Results

#### 3.1. Several mixtures of pollutants exert synergistic effects that affect REH cell survival

Using a factorial design, we evaluated the effects of the combination of two pollutants on REH cells, considering seven pollutants (BPA, BADGE, DBP, DEHP, PFOA, OMC and TCEP) at five concentrations ranging from 1 nM to 100 μM (Table 2). Control cells and cells exposed to individual pollutants at each concentration served as benchmarks. In total, 336 pollutant combinations were tested (Supplementary file 1).

In general, many of the individual pollutants at low concentrations (1 nM and 10 nM) increased cell proliferation, whereas higher concentrations resulted in increased cell death (100 μM) (Supplementary file 1). Exposure to individual BPA, BADGE, DBP and OMC resulted in significant reductions in cell viability ( $p < 0.05$ ) only at the highest concentration tested (100 μM), compared to untreated control and vehicle-only treated cells. At lower concentrations, no significant effects were observed. In contrast, combinations of these same pollutants caused a significant decrease in cell viability at concentrations as low as 100 nM. In contrast, most of the pollutant mixtures promoted cell death (202 of 336 pollutant combinations), although the degree may have been less or greater compared to their individual constituents. Based on Bliss Index calculations derived from cell survival data, we observed that a significant proportion of the combinations showed some degree of synergy (284 combinations), while a smaller number showed additive (28 combinations) or antagonistic (24 combinations) interactions in promoting REH cell death (Table 2). Despite the high incidence of synergistic interactions, their effects were generally mild, with 108 combinations showing a Bliss Index of  $< 10$ .

The ten pollutant combinations that showed the highest Bliss Index (32.0–41.4) for synergy mainly involved BPA and BADGE, combined with DBP or DEHP. In particular, most of these interactions occurred when one pollutant at 1 nM was combined with another at 10 nM, similar to levels commonly detected in the environment. Meanwhile, the ten mixtures with the most negative Bliss index (−8.9 to −4.2), indicating antagonistic effects, primarily involved DEHP combined with OMC or PFOA. However, these antagonistic effects were mostly observed at concentrations of 100 μM or higher. Combinations that showed additive effects were predominantly associated with BADGE at high concentrations (100 μM), particularly when paired with other endocrine disrupting compounds (Table 2).

#### 3.2. Pollutants alter gene expression in flies and their analysis suggests that BPA-DBP-OMC and BADGE-OMC-TCEP mixtures have deleterious effects at NOEL concentrations

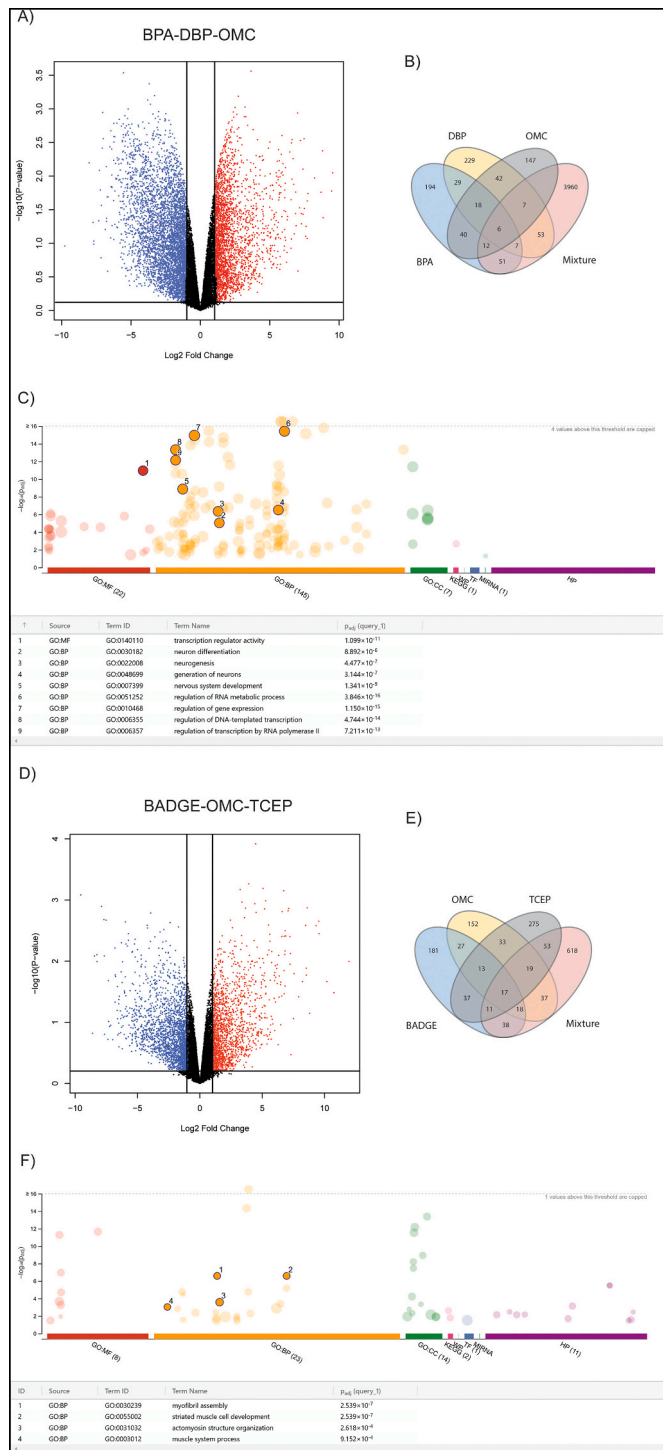
After identifying these synergistic interactions, we further investigated the mechanisms of pollutant interactions by studying their effects in the model organism *Drosophila melanogaster*. The study examined the transcriptional effects of 40 pollutant combinations on the NOEL concentrations of their individual components (Table 3). In addition, the effects of individual pollutants at the same NOEL concentrations, together with the corresponding controls, were also evaluated for comparison. All the combinations produced differentially expressed genes in varying amounts (Supplementary file 2). In most pollutant combinations, we identified between 25 and 40 differentially expressed genes, as detailed in Supplementary Table 1. Notably, the majority of these combinations exhibited a greater number of upregulated genes compared to downregulated ones. Each combination showed a unique pattern of gene regulation, highlighting the specificity of their interactions. Among all combinations, BPA-DBP-OMC and BADGE-OMC-TCEP stood out as the most significant, showing the greatest impact on gene expression.

The BPA-DBP-OMC combination resulted in the highest number of differentially expressed genes, with a total of 4127 genes (Fig. 1A).

**Table 3**  
Combinations of pollutants analyzed in flies.

	BADGE 1 μM	DBP 15 nM	DEHP 20 μM	PFOA 10 μM	4MBC 1 μM	OMC 1 μM
	X					DBP 15 nM
	X	X				DEHP 20 μM
BPA 3 nM	X	X	X			PFOA 10 μM
		X	X	X		4MBC 1 μM
	X	X	X	X		OMC 1 μM
	X			X	X	TCEP 10 nM
		X	X			PFOA 10 μM
BADGE 1 μM		X	X	X		4MBC 1 μM
			X	X	X	OMC 1 μM
			X		X	TCEP 10 nM
			X	X		PFOA 10 μM
DBP 15 nM			X	X		4MBC 1 μM
			X	X	X	OMC 1 μM
			X	X		TCEP 10 nM
DEHP 20 μM					X	TCEP 10 nM
PFOA 10 μM					X	OMC 1 μM
4MBC 1 μM						X
						TCEP 10 nM

Among them, 1849 genes were downregulated and 2278 were upregulated. Although some of these genes overlapped with those affected by individual pollutants, most were unique to the combination (Fig. 1B). GO enrichment analysis revealed that the upregulated genes were strongly associated with transcriptional regulation, including processes such as transcriptional regulatory activity ( $p \text{ adj} = 1.099 \times 10^{-11}$ ), regulation of RNA metabolic processes ( $p \text{ adj} = 3.846 \times 10^{-16}$ ), regulation of gene expression ( $p \text{ adj} = 1.150 \times 10^{-15}$ ), regulation of DNA-templated transcription ( $p \text{ adj} = 4.744 \times 10^{-14}$ ) and regulation of transcription by RNA polymerase II ( $p \text{ adj} = 7.211 \times 10^{-14}$ ). In addition, more subtle effects were observed in neurodevelopment-related processes, such as nervous system development ( $p \text{ adj} = 1.341 \times 10^{-9}$ ) (The differentially expressed genes associated with this process were Ex, HSPC300, Ecd, CSN4, Spdo, Manf, Liprin-Gamma, Nf-YC, Dbo, Dsx, Pnt, Frac, CG10431, Ptc, Dar1, Simj, Mtl, Dscam1, Tws, SMC3, Cyct, Sema1b, Patj, Nf-YA, Rau, Gicat-P, Ari-1, CG10365, Mav, Br, Nlg1, Pex1, Sol, Ab, Vvl, Ssh, Pk, Dad, Su(Z)12, Eps-15, Wts, Pon, Numb, Da, Qless, Reph, Sema1a, Kis, Mbs, Sick, Pod1, Brat, Ptp99A, Ds, Spn-F, Vav, Pdm3, Chic, Sav, 14-3-3epsilon, Mgr, Doa, Rhogef64c, CG12935, Caup, Mam, Osa, Fs(1)H, Svp, Zfh1, Kibra, Cpb, Nudc, Arpc1, Atf3, Pcx, Ptp61F, Enok, Rip11, CG8668, Wg, Ham, Frtz, Psc, So, Mob4, Dpp, Pka-C1, Rac1, Rab8, Cdi, Ire1, Lmx1a, Atx2, Nkd, Fray, Robo1, Mob2, Ena, Shn, Mtg, Spri, Beat-Vc, Lmd, Csw, Bx, Snr1, Ru, Wasp, Lim3, Tgo, MAGE, Dsor1, Capt, B-H2, Nmo, Cato, Cyce, CG8765, Glec, Dap160, Futsch, βTub60D, and Shf), neurite generation ( $p \text{ adj} = 3.144 \times 10^{-7}$ ) (The differentially expressed genes associated with this process were Ex, HSPC300, Ecd, CSN4, Spdo, Manf, Liprin-Gamma, Nf-YC, Dbo, Dsx, Pnt, Frac, CG10431, Ptc, Dar1, Simj, Mtl, Dscam1, Tws, SMC3, Cyct, Sema1b, Patj, Nf-YA, Rau, Gicat-P, Ari-1, CG10365, Mav, Br, Nlg1, Pex1, Sol, Ab, Vvl, Ssh, Pk, Dad, Su(Z)12, Eps-15, Wts, Pon, Numb, Da, Qless, Reph, Sema1a, Kis, Mbs, Sick, Pod1, Brat, Ptp99A, Ds, Spn-F, Vav, Pdm3,



(caption on next column)

**Fig. 1. Synergistic effects of pollutant mixtures on gene expression.** (A) Volcano plot illustrating the genes synergistically overexpressed (red dots) and underexpressed (blue dots) in the BPA-DBP-OMC mixture compared to treatments with individual pollutants and controls. (B) Venn diagrams showing overlap of differentially expressed genes across exposures to BPA, DBP, OMC, or their mixture. (C) GO enrichment analysis of all upregulated differentially expressed genes identified in the BPA-DBP-OMC mixture. The highlighted GO terms were specifically selected because they informed the design of subsequent experiments. For the BPA-DBP-OMC combination, the selected GO terms are related to neurodevelopmental processes, including nervous system development, neurite formation, neurogenesis, and neuronal differentiation. An adjusted  $p$ -value threshold of  $10^{-4}$  was applied in the selection of these terms. (D) Volcano plot displaying genes synergistically overexpressed (red dots) and underexpressed (blue dots) in the BADGE-OMC-TCEP mixture relative to individual treatments and controls. (E) Venn diagrams highlighting overlaps of differentially expressed genes for exposures to BADGE, OMC, TCEP, or their mixture. (F) GO enrichment analysis of all upregulated differentially expressed genes identified in the BADGE-OMC-TCEP mixture. The highlighted GO terms were specifically selected because they informed the design of subsequent experiments. In the case of the BADGE-OMC-TCEP combination, the enriched terms pertain to muscle-related functions, such as muscle cell development, myofibril assembly, actomyosin structure organization, and broader muscle system processes. An adjusted  $p$ -value threshold of  $10^{-4}$  was applied in the selection of these terms.

Chic, Sav, 14-3-3epsilon, Mgr, Doa, Rhogef64c, CG12935, Caup, Mam, Osa, Fs(1)H, Svp, Zfh1, Kibra, Cpb, Nudc, Arpc1, Atf3, Pcx, Ptp61F, Enok, Rip11, CG8668, Wg, Ham, Frtz, Psc, So, Mob4, Dpp, Pka-C1, Rac1, Rab8, Cdi, Ire1, Lmx1a, Atx2, Nkd, Fray, Robo1, Mob2, Ena, Shn, Mtg, Spri, Beat-Vc, Lmd, Csw, Bx, Snr1, Ru, Wasp, Lim3, Tgo, MAGE, Dsor1, Capt, B-H2, Nmo, Cato, Cyce, CG8765, Glec, Dap160 and Shf), neurogenesis ( $p_{adj} = 4.477 \times 10^{-7}$ ) (The differentially expressed genes associated with this process were Ex, CSN4, Manf, Liprin-Gamma, NF-YC, Dsx, Pnt, Frac, CG10431, Ptc, Dar1, Mtl, Dscam1, Tw5, SMC3, Sema1b, Patj, Nf-YA, Rau, Ari-1, CG10365, Mav, Br, Pex1, Ab, Vvl, Ssh, Pk, Dad, Su(Z)12, Wts, Pon, Numb, Da, Qless, Sema1a, Kis, Mbs, Sick, Pod1, Brat, Ptp99A, Ds, Spn-F, Vav, Pdm3, Chic, Sav, 14-3-3epsilon, Mgr, Doa, Rhogef64c, Caup, Mam, Osa, Fs(1)H, Svp, Zfh1, Kibra, Nudc, Arpc1, Ptp61F, Enok, Rip11, CG8668, Wg, Ham, Frtz, So, Mob4, Dpp, Pka-C1, Rac1, Cdi, Ire1, Lmx1a, Atx2, Nkd, Robo1, Mob2, Ena, Shn, Spri, Beat-Vc, Csw, Snr1, Ru, Wasp, Lim3, Tgo, MAGE, Dsor1, Capt, B-H2, Cato, Cyce, CG8765, Dap160, Futsch,  $\beta$ Tub60D and Shf) and neuronal differentiation ( $p_{adj} = 8.902 \times 10^{-8}$ ) (The differentially expressed genes associated with this process were Ex, CSN4, Manf, Liprin-Gamma, NF-YC, Dsx, Pnt, Frac, CG10431, Ptc, Dar1, Mtl, Dscam1, SMC3, Sema1b, Patj, Nf-YA, Rau, Mav, Br, Ab, Vvl, Ssh, Pk, Dad, Wts, Da, Sema1a, Kis, Mbs, Sick, Pod1, Brat, Ptp99A, Ds, Spn-F, Vav, Pdm3, Chic, Sav, 14-3-3epsilon, Doa, Rhogef64c, Caup, Mam, Osa, Fs(1)H, Svp, Zfh1, Kibra, Nudc, Arpc1, Ptp61F, Rip11, CG8668, Wg, Ham, Frtz, Psc, So, Mob4, Dpp, Pka-C1, Rac1, Cdi, Ire1, Lmx1a, Atx2, Robo1, Mob2, Ena, Shn, Spri, Beat-Vc, Csw, Snr1, Ru, Wasp, Lim3, Tgo, Dsor1, Capt, B-H2, Cato, Cyce, CG8765, Futsch,  $\beta$ Tub60D and Shf). In contrast, down-regulated genes mainly indicated a link to methyltransferase activity ( $p_{adj} = 7.965 \times 10^{-6}$ ) (Differentially expressed genes associated with this process were CG9154, SMYDA-4, SMYDA-3, SMYDA-9, CG33230, CG3137, CG11109, CG3337, CG7544, CG14100, CG14618, CG3793, CG18048, HEN1, CG12863, CG17219, CG2614, ART6, CG11447, CG5220, Su(VAR)3-9, CG9386, METTL14, Csu1, CG17807, CG188853, Agt, CG9249, CG2453, NTMT, NSUN2, CG4300, FIB, CG5339 and CG12822) (Fig. 1C).

The BADGE-OMC-TCEP combination resulted in 811 differentially expressed genes, of which 249 were downregulated and 562 were upregulated (Fig. 1D). Similar to the previous case, although some of these genes were coincident with those affected by individual pollutants, most were unique to the combination (Fig. 1E). GO enrichment analysis revealed that the upregulated genes were strongly associated with muscle function, including processes such as muscle cell development ( $p$

adj =  $2.539 \times 10^{-7}$ ) (The differentially expressed genes associated with this process were Mhc, Prm, Tm2, Up, Unc-89, Mlc2, Zasp67, Tmod, Tn, Mlp84B, Bt, Prm and Wupa), myofibril assembly ( $p$  adj =  $2.539 \times 10^{-7}$ ) (The differentially expressed genes associated with this process were Mhc, Prm, Tm2, Up, Unc-89, Mlc2, Zasp67, Tmod, Tn, Mlp84B, Bt, Prm and Wupa), actomyosin structure organization ( $p$  adj =  $2.618 \times 10^{-4}$ ) (The differentially expressed genes associated with this process were Mhc, Prm, Tm2, Up, Tm1, Unc-89, Mlc2, Zasp67, Tmod, Tn, Mlp84B, Bt and Wupa), and muscle system processing ( $p$  adj =  $9.152 \times 10^{-4}$ ) (The differentially expressed genes associated with this process were Mlc1, Mhc, Tm2, Up, Tm1, Unc-89, Mlc2, Tn and Wupa) (Fig. 1F). In contrast,

the downregulated genes did not show a large enrichment in a specific category, with only a subtle link to serine hydrolase activity ( $p$  adj =  $8.190 \times 10^{-3}$ ) (The differentially expressed genes associated with this process were CG10232, Jon66Ci, Jon66Cii, CG32376, CG1304, Gas, Jhedup, CG19764, CG31205, CG11309, CG43336, Gammatriv, CG7179, Ser6, Ser8, CG6592 and CG4053).

3.3. BPA-DBP-OMC and BADGE-OMC-TCEP mixtures did not show a significant change in locomotion or sleep behavior at NOEL concentrations

Given the evidence pointing to effects on neural and muscle

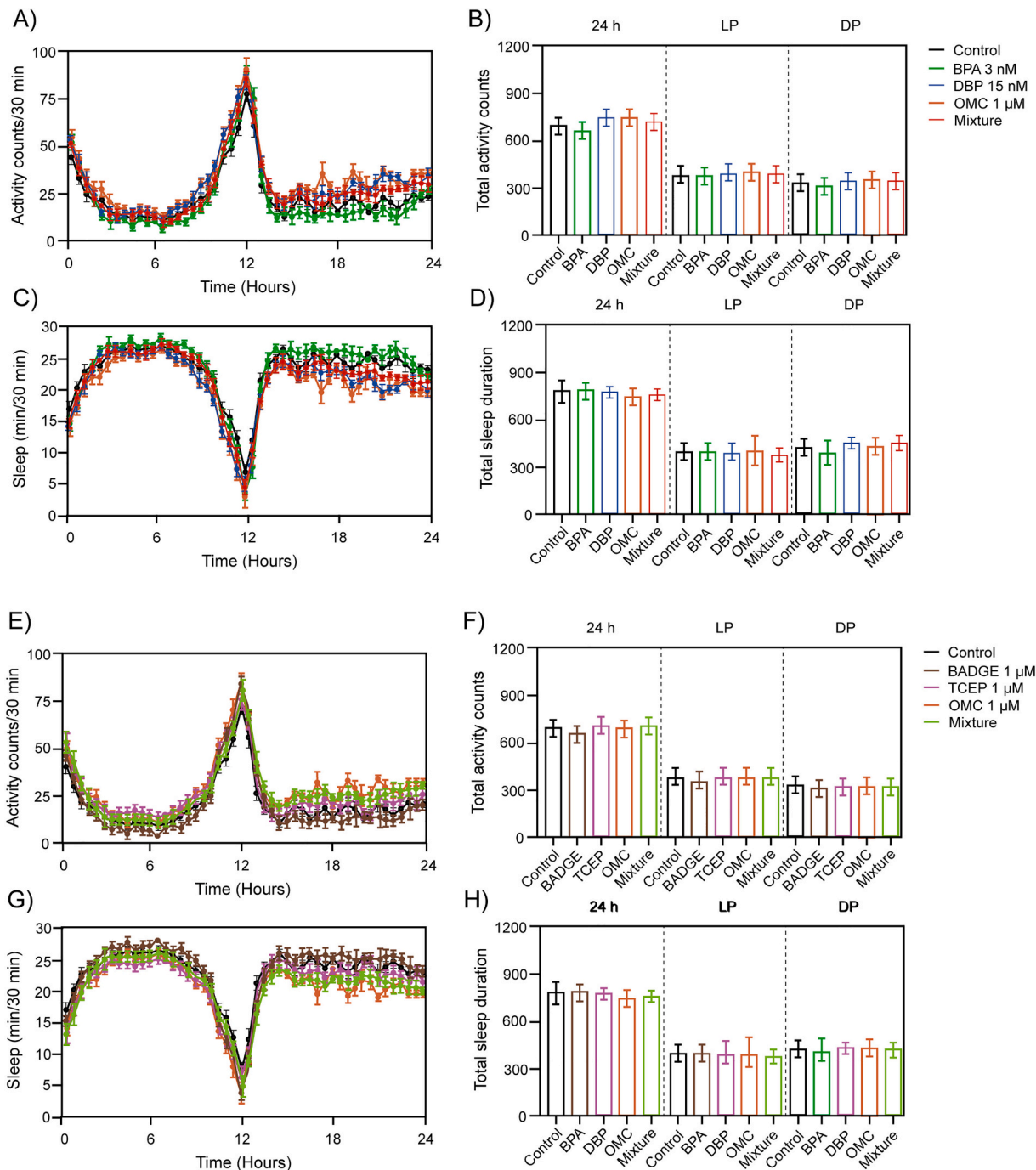


**Fig. 2.** Effects of pollutant mixtures on locomotor activity and sleep patterns. Flies were reared for 10 days on food containing the BPA-DBP-OMC mixture (Panels A-D), the BADGE-OMC-TCEP mixture (Panels E-H) or individual pollutants. During a 24-h period, their locomotor activity and sleep patterns were recorded. The results show the mean locomotor activity (A and E), sleep patterns (C and G), total activity counts (B and F) and total sleep time (D and H) for each group. However, no significant differences were observed in any of the groups, indicating that the exposures did not affect the movement or sleep of the flies.

development, we sought to determine whether the effects of the BPA-DBP-OMC and BADGE-OMC-TCEP mixtures are reflected in the locomotor activity or sleep patterns of flies. The average locomotor activity and sleep patterns of flies exposed to the aforementioned mixtures, individual pollutants and the control were measured. Total activity counts and total sleep duration were also evaluated. Although some changes were observed between treatments, none of these alterations were statistically significant for any of the variables analyzed (Fig. 2).

### 3.4. BPA-DBP-OMC impair neuronal differentiation, while BADGE-OMC-TCEP delays muscle differentiation

To perform a more specific analysis and determine whether the effects observed in flies also apply to mammalian cells, two differentiating cell lines were selected: one for neuronal differentiation and one for muscle differentiation. Differentiation markers of each cell line were analyzed to assess the effects during differentiation protocols. *Drosophila* homologs of MAP2 (Futsch) and  $\beta$ II-tubulin ( $\beta$ Tub60D) were differentially expressed following exposure to the BPA-DBP-OMC mixture. Similarly, *Drosophila* homolog of myosin heavy chain (mhc) showed differential expression after exposure to the BADGE-OMC-TCEP mixture.

After exposing the NTERA-2 cl.D1 cells to retinoic acid, alone or in combination with individual pollutants or with the BPA-DBP-OMC mixture, a delay in the differentiation process was observed. Specifically, MAP2 protein, associated with dendrite development, was not expressed in cells exposed to the mixture, whereas it was expressed in the positive control group and in the group exposed to individual BPA, DBP and OMC. In contrast,  $\beta$ III-tubulin was expressed in all treatment groups, although at varying levels. Nestin expression was only detected in the negative control cells, which were not exposed to any pollutant or retinoic acid, indicating that they did not undergo differentiation (Fig. 3A).

In C2C12 cells, application of the differentiation protocol with

exposure to the BADGE-OMC-TCEP mixture resulted in a delay in the differentiation process. This delay was evident as myosin heavy chain, a key marker of muscle fibers, was not expressed in cells exposed to the mixture, individual TCEP or OMC. In contrast, MHC expression was observed in the positive control group and individual BADGE. Desmin, a protein associated with muscle development, was expressed in all treatment groups, although at variable levels. PAX7, a marker of undifferentiated muscle progenitor cells, was only detected in the negative control group, in which cells were not exposed to any pollutant or the differentiation protocol (Fig. 3B).

## 4. Discussion

The findings presented here reveal that synergistic interactions between pollutants are much more frequent than previously recognized, even at concentrations traditionally considered innocuous. The selection of concentration ranges for some of the pollutants analyzed was based on our previous results in cytotoxicity testing (Lagunas-Rangel et al., 2023). For other compounds, concentrations were chosen based on the literature, which typically describes environmental levels, detected in soil, water and occasionally in biological samples, ranging from the nanomolar to micromolar scale (Owczarek et al., 2022; Philip et al., 2018; Surenjav et al., 2022).

In particular, we highlighted two mixtures, BPA-DBP-OMC and BADGE-OMC-TCEP, which led to a marked reduction in the expression of protein markers of neuronal (MAP2) and muscle (myosin heavy chain) differentiation, respectively. In particular, the presence of the BPA-DBP-OMC mixture has been reported in commercial water, although it has not been associated with any disease (da Silva Costa and Fernandes, 2021). All of this further underscore the importance of further development of such study approaches using combinations of pollutants.

Notably, the BPA-DBP-OMC combination altered substantially more

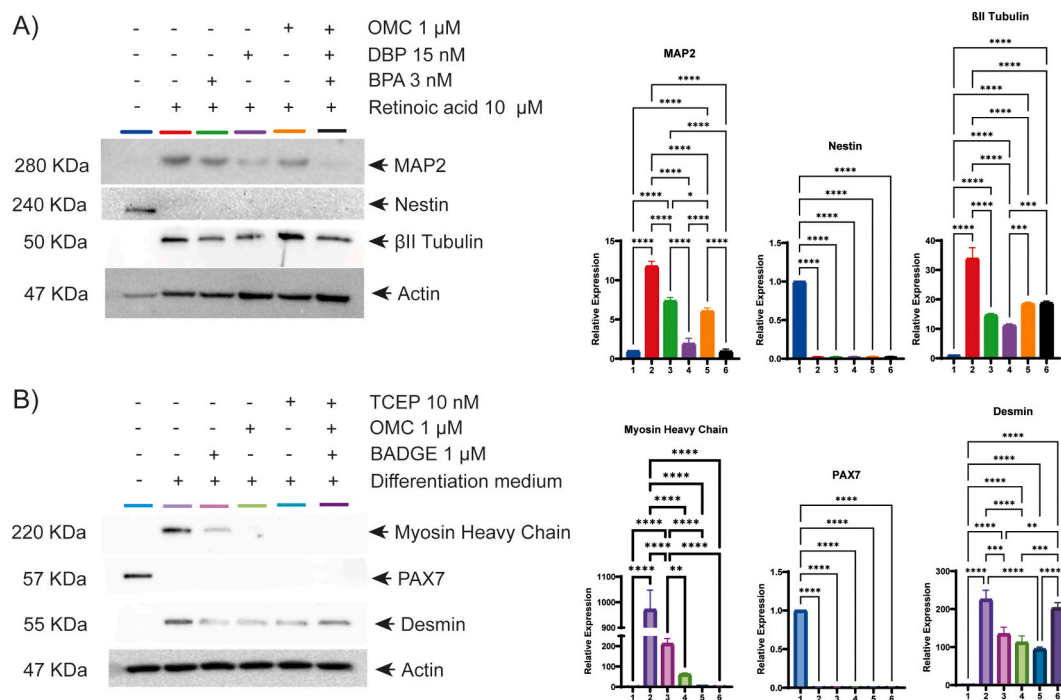


**Fig. 3. Effects of BPA-DBP-OMC and BADGE-OMC-TCEP mixtures on cell differentiation.** A) Representative western blot showing the effects of the BPA-DBP-OMC mixture and its individual components on the expression of three key markers involved in neuronal differentiation of NTERA-2 cl.D1 cells (MAP2, nestin and  $\beta$ III tubulin). The densitometric analysis for each marker is also shown ( $n = 3$ ). B) Representative western blot analysis illustrating the effects of the BADGE-OMC-TCEP mixture and its individual components on the expression of three markers associated with muscle differentiation in C2C12 cells (MHC, PAX7 and desmin). The densitometric analysis for each marker is also shown ( $n = 3$ ). Normality of the data was assessed by the Shapiro-Wilk test. For comparisons between groups, one-way analysis of variance (ANOVA) followed by Tukey's post hoc. \*  $p$  value  $\leq 0.05$ , \*\*  $p$  value  $\leq 0.01$ , \*\*\*  $p$  value  $\leq 0.001$ , \*\*\*\*  $p$  value  $\leq 0.0001$ .

genes compared to the other combinations (approximately 4000 SDRs vs. 20–40 SDRs). One possible explanation for this pronounced effect is the estrogenic activity of both BPA and DBP. When acting synergistically, these compounds can activate estrogen receptors (Mileo et al., 2023; Yuan et al., 2023), which are known to regulate a wide range of genes, including those encoding transcription factors, potentially amplifying the downstream effects on global gene expression.

The pollutant combinations that showed the most significant cytotoxic synergy highlight the potentiating effects of bisphenol derivatives and phthalates. This relationship has already been observed in our previous studies using other cell lines (HeLa) (Jatkowska et al., 2021) as well as by other investigators (Tassinari et al., 2021). Joint exposure to BPA and DBP has been shown to increase cytotoxicity by causing oxidative stress (Sonavane and Gassman, 2019). Furthermore, this combination increases the apoptotic susceptibility of pancreatic  $\alpha$  cells through activation of HSP60/caspase-3 signaling (Morsi et al., 2022). Similarly, combined exposure to BPA and DEHP leads to alterations in oxidant/antioxidant balance and expression of endoplasmic reticulum stress markers (Ozkemahli et al., 2022). Furthermore, this combination promotes tumorigenesis through the regulation of key signaling pathways, including ESR1/HDAC6/PTEN and c-MYC, which are involved in cell survival and proliferation (Zhang et al., 2022; Zhang et al., 2021).

Regarding the genes found to be differentially expressed in *Drosophila*, it is important to note that many of them are species-specific and do not have direct human homologs. In the cases where homologous genes exist in humans, most have not yet been investigated in the context of environmental pollutants. Notably, most of the existing findings regarding the effects of these compounds are on BPA. In *Drosophila*, the *Manf* gene, known to encode a protein that selectively supports dopaminergic neuron survival, was significantly upregulated following exposure to the BPA-DBP-OMC mixture. This aligns with previous findings in *Danio rerio*, where *Manf* was also overexpressed after exposure to BPA at 1500 ng/L (Heredia-García et al., 2023). Additionally, BPA and DBP have each been reported to affect the expression of *DMRT1*, a homolog of the *Drosophila* gene *Dsx*, which also showed altered expression in our study (Jobling et al., 2011; Yang et al., 2018). Mice prenatal exposure to BPA at 5 mg/kg/day has been shown to alter the expression of *NfyA* in adipose tissue (Shu et al., 2019). BPA has been shown to upregulate *CCNE1*, a gene involved in cell cycle regulation, while simultaneously inhibiting follicle growth and inducing atresia in mouse antral follicles (Peretz et al., 2012). In our study, the *Drosophila* homolog of *CCNE1*, *Cyce*, also exhibited differential expression following exposure to the BPA-containing mixture. Moreover, BPA reduces the expression of *NeuroD1*, a key transcription factor in neuronal differentiation (Suresh and Vellapandian, 2024). We identified changes in the expression of the *Drosophila* gene *Tgo*, which is the homolog of *ARNT*, a transcription factor that dimerizes with AhR. This is consistent with previous findings linking BPA exposure to alterations in AhR pathway components in rat models (Merii et al., 2022).

On the other hand, on *Drosophila*, myosin heavy chain (*Mhc*) and troponin (*Tn*) were among the differentially expressed genes after BADGE-OMC-TCEP exposure. However, we have not found similar data reported previously. Interestingly, it has been reported that BPA, precursor of BADGE, at concentrations ranging from 1000 to 10,000 nM, reduces the levels of these proteins in cardiomyocytes by inhibiting the Akt signaling pathway (Go et al., 2018).

BPA, DBP and OMC are chemicals that are known to disrupt endocrine and cellular processes, which can significantly impair the signaling pathways required for proper neuronal differentiation (Naffaa et al., 2021). BPA, which mimics estrogen, can bind to estrogen receptors and alter gene expression, potentially disrupting this vital process. Studies have shown that even low doses of BPA can impair neuronal differentiation in human neural stem/progenitor cells (Kiso-Farnè et al., 2022) and impair the development of GABAergic neurons (Fukushima and Nagao, 2018). In addition, BPA has been found to suppress the differentiation of dopaminergic neurons by downregulating the expression of

IGF-1 (Huang et al., 2017), which is critical for neuronal growth and survival (Bhalla et al., 2022). On the other hand, both DBP and OMC can also interfere with hormonal signaling pathways, which could amplify the harmful effects of BPA. In particular, DBP has been shown to affect neural progenitor cell proliferation and hippocampal neurogenesis, processes essential for brain development (Lee et al., 2019). Furthermore, DBP has been reported to disrupt neuronal maturation in primary cultures of rat embryos, further demonstrating its adverse effects on neuronal differentiation (Lee et al., 2022). Lastly, BPA, BADGE and DBP can interact with other compounds, potentially increasing their bioaccumulation in the body (Sharma et al., 2020). TCEP has been reported to delay mesoderm differentiation in vitro at 250 nM (Kanda and Iwata, 2024).

Similar to the previous case, BADGE, OMC and TCEP are endocrine disruptors and can interact in multiple ways to impair muscle development, including altering gene expression, disrupting signaling pathways and inducing oxidative stress. This is the first report suggesting detrimental muscle effects of OMC and BADGE. Since BADGE is derived from BPA, it is likely to produce similar effects on muscle development. TCEP has been shown to accumulate in salmon muscle with minimal biotransformation in the liver, resulting in steroidogenic responses (Arukwe et al., 2018; Arukwe et al., 2016). The combined presence of these pollutants could create a more toxic environment, with overlapping actions that hinder muscle development.

Furthermore, all of the pollutants that showed synergy in this study can interact with AhR, consequently affecting androgen and estrogen receptor signaling (Banerjee et al., 2023; Wójtowicz et al., 2019; Wójtowicz et al., 2017). In particular, some of these pollutants have a higher affinity for AhR than for androgen and estrogen receptors (Banerjee et al., 2023; Wójtowicz et al., 2019). The effects on AhR signaling have been linked to BPA-induced pancreatic islet toxicity (Banerjee et al., 2023), BADGE-induced sensitization to cellular cytotoxicity (Wójtowicz et al., 2019), as well as DBP-induced apoptosis and neurotoxicity (Wójtowicz et al., 2017). Alterations in AhR signaling also modify the expression of cytochrome P450 subunits, leading to increased ROS production. Chemicals such as BPA (Gassman, 2017), BADGE (Neri et al., 2024), DBP (Wójtowicz et al., 2017), OMC and TCEP (Zhang et al., 2023) have been shown to elevate ROS levels, which could act synergistically to alter cellular redox balance. This alteration could explain the observed reductions in cell viability and alterations in cell differentiation. Furthermore, since ROS naturally increase during muscle (Malinska et al., 2012) and neuronal (Vieira et al., 2011) differentiation, these cells may be particularly vulnerable to sudden fluctuations induced by environmental pollutants.

It is important to note that most studies that have investigated the neuronal and muscular effects of BPA, BADGE, DBP, OMC and TCEP have used significantly higher concentrations, than those reported in this study, which are environmentally relevant. Regarding the differences observed between the results in cell lines and the *Drosophila* model, it is possible that the concentration of pollutant mixtures reaching the muscles and brain of flies is not sufficient to cause significant effects. This could be due to biotransformation processes that reduce their availability, or because pollutants accumulate more in other organs such as fat bodies, stomach and intestines. In addition, physiological barriers such as the blood-brain barrier may further limit their impact. In contrast, cell lines directly exposed to pollutant mixtures lack these protective mechanisms, which could lead to more pronounced effects. It should also be noted that not all cell lines are metabolically competent, which means that they can only manifest the effects of the parent compound. In contrast, whole organisms can metabolize substances into active metabolites, which may also contribute to the observed effects. It is also possible that any damage caused in flies is rapidly repaired, or that the duration of exposure was not long enough to observe appreciable alterations in locomotion or sleep behavior.

Supplementary data to this article can be found online at <https://doi.org/10.1016/j.scitotenv.2025.179848>.

## CRedit authorship contribution statement

**Francisco Alejandro Lagunas-Rangel:** Writing – review & editing, Writing – original draft, Visualization, Validation, Supervision, Methodology, Investigation, Formal analysis, Data curation. **Martin Åberg:** Methodology, Investigation. **Sifang Liao:** Validation, Methodology, Investigation. **Felippe Espinelli-Amorim:** Writing – review & editing, Software, Methodology, Investigation, Data curation. **Rajanidevi Tummaramatti-Hanumant:** Methodology, Investigation. **Ludmila Jackevića:** Methodology. **Monta Briviba:** Writing – review & editing, Methodology, Investigation. **Wen Liu:** Methodology, Investigation. **Robert Fredriksson:** Writing – review & editing, Conceptualization. **Ahmed M. Alsehli:** Writing – review & editing, Methodology, Investigation. **Ola Spjuth:** Writing – review & editing, Conceptualization. **Janis Klovinis:** Writing – review & editing, Methodology, Investigation. **Maija Dambrova:** Writing – review & editing, Resources. **Blažej Kudlak:** Writing – review & editing, Methodology, Investigation, Data curation. **Claes Andersson:** Writing – review & editing, Methodology, Investigation, Conceptualization. **Helgi B. Schiöth:** Writing – review & editing, Supervision, Resources, Project administration, Funding acquisition, Conceptualization.

## Funding

HBS is supported by the Swedish Cancer Society (grants 20090 Pj, and 23 3033 PJ), the Swedish Research Council (Vetenskapsrådet 2022–00562) and the Novo Nordisk Foundation (Novo Nordisk Fonden).

## Declaration of competing interest

The authors declare no conflict of interest.

## Data availability

Data will be made available on request

## References

- Arukwe, A., Carteny, C.C., Eggen, T., Möder, M., 2018. Novel aspects of uptake patterns, metabolite formation and toxicological responses in Salmon exposed to the organophosphate esters—Tris(2-butoxyethyl)- and tris(2-chloroethyl) phosphate. *Aquat. Toxicol.* 196, 146–153. <https://doi.org/10.1016/j.aquatox.2018.01.014>.
- Arukwe, A., Carteny, C.C., Möder, M., Bonini, A., Maubach, M.A., Eggen, T., 2016. Differential modulation of neuro- and interrenal steroidogenesis of juvenile salmon by the organophosphates - tris(2-butoxyethyl)- and tris(2-chloroethyl) phosphate. *Environ. Res.* 148, 63–71. <https://doi.org/10.1016/j.envres.2016.03.020>.
- Banerjee, O., Singh, S., Prasad, S.K., Bhattacharjee, A., Seal, T., Mandal, J., Sinha, S., Banerjee, A., Maji, B.K., Mukherjee, S., 2023. Exploring aryl hydrocarbon receptor (AHR) as a target for bisphenol-a (BPA)-induced pancreatic islet toxicity and impaired glucose homeostasis: protective efficacy of ethanol extract of *Centella asiatica*. *Toxicology* 500, 153693. <https://doi.org/10.1016/j.tox.2023.153693>.
- Bhalla, S., Mehan, S., Khan, A., Rehman, M.U., 2022. Protective role of IGF-1 and GLP-1 signaling activation in neurological dysfunctions. *Neurosci. Biobehav. Rev.* 142, 104896. <https://doi.org/10.1016/j.neubiorev.2022.104896>.
- Blom, K., Nygren, P., Alvarsson, J., Larsson, R., Andersson, C.R., 2016. Ex vivo assessment of drug activity in patient tumor cells as a basis for tailored cancer therapy. *SLAS Technol.* 21, 178–187. <https://doi.org/10.1177/2211068215598117>.
- Bolger, A.M., Lohse, M., Usadel, B., 2014. Trimmomatic: a flexible trimmer for Illumina sequence data. *Bioinformatics* 30, 2114–2120. <https://doi.org/10.1093/bioinformatics/btu170>.
- Boobis, A., Budinsky, R., Collie, S., Crofton, K., Embry, M., Felton, S., Hertzberg, R., Kopp, D., Mihlan, G., Mumtaz, M., Price, P., Solomon, K., Teuschler, L., Yang, R., Zaleski, R., 2011. Critical analysis of literature on low-dose synergy for use in screening chemical mixtures for risk assessment. *Crit. Rev. Toxicol.* 41, 369–383. <https://doi.org/10.3109/10408444.2010.543655>.
- Bopp, S.K., Barouki, R., Brack, W., Dalla Costa, S., Dorne, J.-L.C.M., Drakvik, P.E., Faust, M., Karjalainen, T.K., Kephapoulos, S., van Klaveren, J., Kolossa-Gehring, M., Kortenkamp, A., Lebre, E., Lettieri, T., Nørgaard, S., Rügge, J., Tarazona, J.V., Trier, X., van de Water, B., van Gils, J., Bergman, Å., 2018. Current EU research activities on combined exposure to multiple chemicals. *Environ. Int.* 120, 544–562. <https://doi.org/10.1016/j.envint.2018.07.037>.
- Brack, W., 2015. The challenge : prioritization of emerging pollutants. *Environ. Toxicol. Chem.* 34, 2181. <https://doi.org/10.1002/etc.3046>.
- Brand, J.A., Aich, U., Yee, W.K.W., Wong, B.B.M., Dowling, D.K., 2024. Sexual selection increases male behavioral consistency in *Drosophila melanogaster*. *Am. Nat.* 203, 713–725. <https://doi.org/10.1086/729600>.
- Cedergreen, N., 2014. Quantifying synergy: a systematic review of mixture toxicity studies within environmental toxicology. *PLoS One* 9, e96580. <https://doi.org/10.1371/journal.pone.0096580>.
- da Silva Costa, R., Fernandes, T., Sainara Maia, De Sousa Almeida, E., Tomé Oliveira, J., Carvalho Guedes, J.A., Julião Zocolo, G., Wagner De Sousa, F., Do Nascimento, R.F., 2021. Potential risk of BPA and phthalates in commercial water bottles: a minireview. *J. Water Health* 19, 411–435. <https://doi.org/10.2166/wh.2021.202>.
- Fukushima, N., Nagao, T., 2018. Exposure to bisphenol a affects GABAergic neuron differentiation in neurosphere cultures. *Neuroreport* 29, 712–717. <https://doi.org/10.1097/WNR.0000000000001021>.
- Fuller, R., Landrigan, P.J., Balakrishnan, K., Bathan, G., Bose-O'Reilly, S., Brauer, M., Caravanos, J., Chiles, T., Cohen, A., Corra, L., Cropper, M., Ferraro, G., Hanna, J., Hanrahan, D., Hu, H., Hunter, D., Janata, G., Kupka, R., Lanphear, B., Lichtveld, M., Martin, K., Mustapha, A., Sanchez-Triana, E., Sandilya, K., Schaeffli, L., Shaw, J., Seddon, J., Suk, W., Téllez-Rojo, M.M., Yan, C., 2022. Pollution and health: a progress update. *Lancet Planet Health* 6, e535–e547. [https://doi.org/10.1016/S2542-5196\(22\)00090-0](https://doi.org/10.1016/S2542-5196(22)00090-0).
- Gassman, N.R., 2017. Induction of oxidative stress by bisphenol a and its pleiotropic effects. *Environ. Mol. Mutagen.* 58, 60–71. <https://doi.org/10.1002/em.22072>.
- Geary, N., 2013. Understanding synergy. *American Journal of Physiology-Endocrinology and Metabolism* 304, E237–E253. <https://doi.org/10.1152/ajpendo.00308.2012>.
- Go, G.-Y., Lee, S.-J., Jo, A., Lee, J.-R., Kang, J.-S., Yang, M., Bae, G.-U., 2018. Bisphenol a and estradiol impede myoblast differentiation through down-regulating Akt signaling pathway. *Toxicol. Lett.* 292, 12–19. <https://doi.org/10.1016/j.toxlet.2018.04.019>.
- Goldoni, M., Johansson, C., 2007. A mathematical approach to study combined effects of toxicants in vitro: evaluation of the bliss independence criterion and the Loewe additivity model. *Toxicol. in Vitro* 21, 759–769. <https://doi.org/10.1016/j.tiv.2007.03.003>.
- Goodson, W.H., Lowe, L., Carpenter, D.O., Gilbertson, M., Manaf Ali, A., de Cerain, Lopez, Salsamendi, A., Lasfar, A., Carnero, A., Azqueta, A., Amedei, A., Charles, A.K., Collins, A.R., Ward, A., Salzberg, A.C., Colacci, A.M., Olsen, A.-K., Berg, A., Barclay, B.J., Zhou, B.P., Blanco-Aparicio, C., Bagloli, C.J., Dong, C., Mondello, C., Hsu, C.-W., Naus, C.C., Yedjou, C., Curran, C.S., Laird, D.W., Koch, D. C., Carlin, D.J., Felsner, D.W., Roy, D., Brown, D.G., Ratovitski, E., Ryan, E.P., Corsini, E., Rojas, E., Moon, E.-Y., Laconi, E., Marongiu, F., Al-Mulla, F., Chiaradonna, F., Darroudi, F., Martin, F.L., Van Schooten, F.J., Goldberg, G.S., Wagemaker, G., Nangami, G.N., Calaf, G.M., Williams, G.P., Wolf, G.T., Koppen, G., Brunborg, G., Lyster, H.K., Krishnan, H., Ab Hamid, H., Yasaei, H., Sone, H., Kondoh, H., Salem, H.K., Hsu, H.-Y., Park, H.H., Koturbash, I., Miousse, I.R., Scovassi, A.I., Klauig, J.E., Vondráček, J., Raju, J., Roman, J., Wise, J.P., Whitfield, J.R., Woodrick, J., Christopher, J.A., Ochieng, J., Martinez-Leal, J.F., Weisz, J., Kravchenko, J., Sun, J., Prudhomme, K.R., Narayanan, K.B., Cohen-Solal, K.A., Moorwood, K., Gonzalez, L., Soucek, L., Jian, L., D'Abronzio, L.S., Lin, L.-T., Li, L., Gulliver, L., McCawley, L.J., Memeo, L., Vermeulen, L., Leyns, L., Zhang, L., Valverde, M., Khatami, M., Romano, M.F., Chapellier, M., Williams, M.A., Wade, M., Manjili, M.H., Leonart, M.E., Xia, M., Gonzalez Guzman, M.J., Karamouzis, M.V., Kirsch-Volders, M., Vaccari, M., Kuemmerle, N.B., Singh, N., Cruickshanks, N., Kleinstreuer, N., van Larebeke, N., Ahmed, N., Ogunkua, O., Krishnakumar, P.K., Vadgama, P., Marignani, P.A., Ghosh, P.M., Ostrosky-Wegman, P., Thompson, P.A., Dent, P., Heneberg, P., Darbre, P., Leung, P.S., Nangia-Makker, P., Cheng, Q.S., Robey, R.B., Al-Temaimi, R., Roy, R., Andrade-Vieira, R., Sinha, R.K., Mehta, R., Vento, R., Di Fiore, R., Ponce-Cusi, R., Dornetschuber-Fleiss, R., Nahta, R., Castellino, R.C., Palorini, R., Hamid, R.A., Langie, S.A.S., Eltom, S.E., Brooks, S.A., Ryeom, S., Wise, S.S., Bay, S.N., Harris, S.A., Papagerakis, S., Romano, S., Pavanello, S., Eriksson, S., Forte, S., Casey, S.C., Luanpitpong, S., Lee, T.-J., Otsuki, T., Chen, T., Massfelder, T., Sanderson, T., Guarnieri, T., Hultman, T., Dormoy, V., Odero-Marah, V., Sabbiseti, V., Maguer-Satta, V., Rathmell, W.K., Engström, W., Decker, W.K., Bisson, W.H., Rojanasakul, Y., Luqmani, Y., Chen, Z., Hu, Z., 2015. Assessing the carcinogenic potential of low-dose exposures to chemical mixtures in the environment: the challenge ahead. *Carcinogenesis* 36, S254–S296. <https://doi.org/10.1093/carcin/bgv039>.
- Heredia-García, G., Elizalde-Velázquez, G.A., Gómez-Oliván, L.M., Islas-Flores, H., García-Medina, S., Galar-Martínez, M., Dublán-García, O., 2023. Realistic concentrations of bisphenol-a trigger a neurotoxic response in the brain of zebrafish: oxidative stress, behavioral impairment, acetylcholinesterase inhibition, and gene expression disruption. *Chemosphere* 330, 138729. <https://doi.org/10.1016/j.chemosphere.2023.138729>.
- Heudorf, U., Mersch-Sundermann, V., Angerer, J., 2007. Phthalates: toxicology and exposure. *Int. J. Hyg. Environ. Health* 210, 623–634. <https://doi.org/10.1016/j.ijheh.2007.07.011>.
- Huang, B., Ning, S., Zhang, Q., Chen, A., Jiang, C., Cui, Y., Hu, J., Li, H., Fan, G., Qin, L., Liu, J., 2017. Bisphenol a represses dopaminergic neuron differentiation from human embryonic stem cells through downregulating the expression of insulin-like growth factor 1. *Mol. Neurobiol.* 54, 3798–3812. <https://doi.org/10.1007/s12035-016-9898-y>.
- Jatkowska, N., Kudlak, B., Lewandowska, P., Liu, W., Williams, M.J., Schiöth, H.B., 2021. Identification of synergistic and antagonistic actions of environmental pollutants: bisphenols a, S and F in the presence of DEP, DBP, BADGE and BADGE-2HCl in three component mixtures. *Sci. Total Environ.* 767, 144286. <https://doi.org/10.1016/j.scitotenv.2020.144286>.
- Jobling, M.S., Hutchison, G.R., van den Driesche, S., Sharpe, R.M., 2011. Effects of di(n-butyl) phthalate exposure on foetal rat germ-cell number and differentiation:

- identification of age-specific windows of vulnerability. *Int. J. Androl.* 34, e386–e396. <https://doi.org/10.1111/j.1365-2605.2010.01140.x>.
- Kanda, K., Iwata, H., 2024. Tris(2-chloroethyl) phosphate (TCEP) exposure inhibits the epithelial-mesenchymal transition (EMT), mesoderm differentiation, and cardiovascular development in early chicken embryos. *Sci. Total Environ.* 922, 171242. <https://doi.org/10.1016/j.scitotenv.2024.171242>.
- Kim, D., Paggi, J.M., Park, C., Bennett, C., Salzberg, S.L., 2019. Graph-based genome alignment and genotyping with HISAT2 and HISAT-genotype. *Nat. Biotechnol.* 37, 907–915. <https://doi.org/10.1038/s41587-019-0201-4>.
- Kiso-Farné, K., Yaoi, T., Fujimoto, T., Itoh, K., 2022. Low doses of bisphenol a disrupt neuronal differentiation of human neuronal stem/progenitor cells. *Acta Histochem. Cytochem.* 55, 22–00090. <https://doi.org/10.1267/ahc.22-00090>.
- Kolberg, L., Raudvere, U., Kuzmin, I., Adler, P., Vilo, J., Peterson, H., 2023. G: profiler—interoperable web service for functional enrichment analysis and gene identifier mapping (2023 update). *Nucleic Acids Res.* 51, W207–W212. <https://doi.org/10.1093/nar/gkad347>.
- Kudlak, B., Jatkowska, N., Liu, W., Williams, M.J., Barcelo, D., Schiöth, H.B., 2022. Enhanced toxicity of bisphenols together with UV filters in Water: identification of synergy and antagonism in three-component mixtures. *Molecules* 27, 3260. <https://doi.org/10.3390/molecules27103260>.
- Lagunas-Rangel, F.A., Kudlak, B., Liu, W., Williams, M.J., Schiöth, H.B., 2022. The potential interaction of environmental pollutants and circadian rhythm regulations that may cause leukemia. *Crit. Rev. Environ. Sci. Technol.* 52, 4094–4112. <https://doi.org/10.1080/10643389.2021.1985882>.
- Lagunas-Rangel, F.A., Linnea-Niemi, J.V., Kudlak, B., Williams, M.J., Jönsson, J., Schiöth, H.B., 2022b. Role of the synergistic interactions of environmental pollutants in the development of Cancer. *Geohealth* 6. <https://doi.org/10.1029/2021GH000552>.
- Lagunas-Rangel, F.A., Liu, W., Schiöth, H.B., 2023. Interaction between environmental pollutants and cancer drug efficacy: bisphenol a, bisphenol a diglycidyl ether and Perfluorooctanoic acid reduce vincristine cytotoxicity in acute lymphoblastic leukemia cells. *J. Appl. Toxicol.* 43, 458–469. <https://doi.org/10.1002/jat.4398>.
- Landrigan, P.J., Fuller, R., Acosta, N.J.R., Aveyi, O., Arnold, R., Basu, N. (Nil), Baldé, A. B., Bertollini, R., Bose-O'Reilly, S., Boufford, J.L., Breyse, P.N., Chiles, T., Mahidol, C., Coll-Seck, A.M., Cropper, M.L., Fobil, J., Fuster, V., Greenstone, M., Haines, A., Hanrahan, D., Hunter, D., Khare, M., Krupnick, A., Lanphear, B., Lohani, B., Martin, K., Mathiasen, K.V., McTeer, M.A., Murray, C.J.L., Ndashimananjara, J.D., Perera, F., Potočnik, J., Preker, A.S., Ramesh, J., Rockström, J., Salinas, C., Samson, L.D., Sandilya, K., Sly, P.D., Smith, K.R., Steiner, A., Stewart, R.B., Suk, W.A., van Schayck, O.C.P., Yadama, G.N., Yumkella, K., Zhong, M., 2018. The lancet commission on pollution and health. *Lancet* 391, 462–512. [https://doi.org/10.1016/S0140-6736\(17\)32345-0](https://doi.org/10.1016/S0140-6736(17)32345-0).
- Lee, S., Lee, W., Yang, S., Suh, Y.J., Hong, D.G., Chang, S.-C., Kim, H.S., Lee, J., 2022. Di-*n*-butyl phthalate disrupts neuron maturation in primary rat embryo neurons and male C57BL/6 mice. *J. Toxicol. Environ. Health A* 85, 56–70. <https://doi.org/10.1080/15287394.2021.1973631>.
- Lee, W., Cho, J.-H., Lee, Y., Lee, S., Kim, D.H., Ha, S., Kondo, Y., Ishigami, A., Chung, H. Y., Lee, J., 2019. Dibutyl phthalate impairs neural progenitor cell proliferation and hippocampal neurogenesis. *Food Chem. Toxicol.* 129, 239–248. <https://doi.org/10.1016/j.fct.2019.04.040>.
- Li, R., Wang, H., Mi, C., Feng, C., Zhang, L., Yang, L., Zhou, B., 2019. The adverse effect of TCIPP and TCEP on neurodevelopment of zebrafish embryos/larvae. *Chemosphere* 220, 811–817. <https://doi.org/10.1016/j.chemosphere.2018.12.198>.
- Liao, S., Sun, C., Lagunas-Rangel, F.A., Liu, W., Yi, S., Browne-Johnson, D., Eklund, F., Zhang, Y., Kudlak, B., Williams, M.J., Schiöth, H.B., 2024. Perfluorooctanoic acid induces transgenerational modifications in reproduction, metabolism, locomotor activity, and sleep behavior in *Drosophila melanogaster* and deleterious effects in human cancer cells. *Sci. Total Environ.* 957, 177472. <https://doi.org/10.1016/j.scitotenv.2024.177472>.
- Liao, Y., Smyth, G.K., Shi, W., 2014. featureCounts: an efficient general purpose program for assigning sequence reads to genomic features. *Bioinformatics* 30, 923–930. <https://doi.org/10.1093/bioinformatics/btt656>.
- Lindhagen, E., Nygren, P., Larsson, R., 2008. The fluorometric microculture cytotoxicity assay. *Nat. Protoc.* 3, 1364–1369. <https://doi.org/10.1038/nprot.2008.114>.
- Liu, W., Cao, H., Liao, S., Kudlak, B., Williams, M.J., Schiöth, H.B., 2021. Dibutyl phthalate disrupts conserved circadian rhythm in *Drosophila* and human cells. *Sci. Total Environ.* 783, 147038. <https://doi.org/10.1016/j.scitotenv.2021.147038>.
- Malinska, D., Kudin, A.P., Bejtka, M., Kunz, W.S., 2012. Changes in mitochondrial reactive oxygen species synthesis during differentiation of skeletal muscle cells. *Mitochondrion* 12, 144–148. <https://doi.org/10.1016/j.mito.2011.06.015>.
- Mauderly, J.L., Samet, J.M., 2009. Is there evidence for synergy among air pollutants in causing health effects? *Environ. Health Perspect.* 117, 1–6. <https://doi.org/10.1289/ehp.11654>.
- Merii, M.H., Fardoun, M.M., El Asmar, K., Khalil, M.I., Eid, A.H., Dhaini, H.R., 2022. Effect of BPA on CYP450s expression, and nicotine modulation, in fetal rat brain. *Neurotoxicol. Teratol.* 92, 107095. <https://doi.org/10.1016/j.ntt.2022.107095>.
- Mileo, A., Chianese, T., Fasciolo, G., Venditti, P., Capalao, A., Rosati, L., De Falco, M., 2023. Effects of Dibutylphthalate and steroid hormone mixture on human prostate cells. *Int. J. Mol. Sci.* 24, 14341. <https://doi.org/10.3390/ijms241814341>.
- Morsi, A.A., Mersal, E.A., Alsabih, A.O., Abdelmoneim, A.M., Sakr, E.M., Alakabawy, S., Elfawal, R.G., Naji, M., Aljanfawe, H.J., Alshateb, F.H., Shawky, T.M., 2022. Apoptotic susceptibility of pancreatic alpha cells to environmentally relevant dose levels of bisphenol-a versus dibutyl phthalate is mediated by HSP60/caspase-3 expression in male albino rats. *Cell Biol. Int.* 46, 2232–2245. <https://doi.org/10.1002/cbin.11909>.
- Naffaa, V., Laprévotte, O., Schang, A.-L., 2021. Effects of endocrine disrupting chemicals on myelin development and diseases. *Neurotoxicology* 83, 51–68. <https://doi.org/10.1016/j.neuro.2020.12.009>.
- Neri, I., Piccolo, M., Russo, G., Ferraro, M.G., Marotta, V., Santamaria, R., Grumetto, L., 2024. The combined use of biological investigations, bio chromatographic and in silico methods to solve the puzzle of badge and its derivative's toxicity. *Chemosphere* 367, 143640. <https://doi.org/10.1016/j.chemosphere.2024.143640>.
- Niu, J., Straubinger, R.M., Mager, D.E., 2019. Pharmacodynamic Drug–Drug Interactions. *Clin. Pharmacol. Ther.* 105, 1395–1406. <https://doi.org/10.1002/cpt.1434>.
- Owczarek, K., Waraksa, E., Klodzińska, E., Zrobok, Y., Ozimek, M., Rachoń, D., Kudlak, B., Wasik, A., Mazerska, Z., 2022. Validated GC–MS method for determination of bisphenol a and its five analogues in dietary and nutritional supplements. *Microchem. J.* 180, 107643. <https://doi.org/10.1016/j.microc.2022.107643>.
- Ozkemahli, G., Erkekoglu, P., Ercan, A., Zeybek, N.D., Yersal, N., Kocer-Gumusel, B., 2022. Effects of single or combined exposure to bisphenol a and mono(2-ethylhexyl) phthalate on oxidant/antioxidant status, endoplasmic reticulum stress, and apoptosis in HepG2 cell line. *Environ. Sci. Pollut. Res.* 30, 12189–12206. <https://doi.org/10.1007/s11356-022-22937-6>.
- Peretz, J., Craig, Z.R., Flaws, J.A., 2012. Bisphenol a inhibits follicle growth and induces atresia in cultured mouse antral follicles independently of the genomic estrogenic Pathway1. *Biol. Reprod.* 87. <https://doi.org/10.1095/biolreprod.112.101899>.
- Philip, J.M., Aravind, U.K., Aravindakumar, C.T., 2018. Emerging contaminants in Indian environmental matrices – a review. *Chemosphere* 190, 307–326. <https://doi.org/10.1016/j.chemosphere.2017.09.120>.
- Poole, A., van Herwijnen, P., Weideli, H., Thomas, M.C., Ransbotyn, G., Vance, C., 2004. Review of the toxicology, human exposure and safety assessment for bisphenol a diglycidylether (BADGE). *Food Addit. Contam.* 21, 905–919. <https://doi.org/10.1080/02652030400007294>.
- Rafeletou, A., Niemi, J.V.L., Lagunas-Rangel, F.A., Liu, W., Kudlak, B., Schiöth, H.B., 2024. The exposure to UV filters: prevalence, effects, possible molecular mechanisms of action and interactions within mixtures. *Sci. Total Environ.* 928, 170999. <https://doi.org/10.1016/j.scitotenv.2024.170999>.
- Ritchie, M.E., Phipson, B., Wu, D., Hu, Y., Law, C.W., Shi, W., Smyth, G.K., 2015. Limma powers differential expression analyses for RNA-seq and microarray studies. *Nucleic Acids Res.* 43, e47. <https://doi.org/10.1093/nar/gkv007>.
- Sharma, M.D., Elanjickal, A.I., Mankar, J.S., Krupadam, R.J., 2020. Assessment of cancer risk of microplastics enriched with polycyclic aromatic hydrocarbons. *J. Hazard. Mater.* 398, 122994. <https://doi.org/10.1016/j.jhazmat.2020.122994>.
- Shu, L., Meng, Q., Diamante, G., Tsai, B., Chen, Y.-W., Mikhail, A., Luk, H., Ritz, B., Allard, P., Yang, X., 2019. Prenatal bisphenol a exposure in mice induces multitissue mitochondrial disruptions linking to Cardiometabolic disorders. *Endocrinology* 160, 409–429. <https://doi.org/10.1210/en.2018-00817>.
- Sonavane, M., Gassman, N.R., 2019. Bisphenol a co-exposure effects: a key factor in understanding BPA'S complex mechanism and health outcomes. *Crit. Rev. Toxicol.* 49, 371–386. <https://doi.org/10.1080/10408444.2019.1621263>.
- Surenjav, E., Lkhasuren, J., Fiedler, H., 2022. POPs monitoring in Mongolia – Core matrices. *Chemosphere* 297, 134180. <https://doi.org/10.1016/j.chemosphere.2022.134180>.
- Suresh, S., Vellapandian, C., 2024. Cyanidin ameliorates bisphenol A-induced Alzheimer's disease pathology by restoring Wnt/ $\beta$ -catenin signaling Cascade: an in vitro study. *Mol. Neurobiol.* 61, 2064–2080. <https://doi.org/10.1007/s12035-023-03672-6>.
- Tassinari, R., Tait, S., Busani, L., Martinelli, A., Valeri, M., Gastaldelli, A., Deodati, A., La Rocca, C., Maranghi, F., 2021. Toxicological assessment of Oral co-exposure to bisphenol a (BPA) and Bis(2-ethylhexyl) phthalate (DEHP) in juvenile rats at environmentally relevant dose levels: evaluation of the synergic, additive or antagonistic effects. *Int. J. Environ. Res. Public Health* 18, 4584. <https://doi.org/10.3390/ijerph18094584>.
- Vieira, H.L.A., Alves, P.M., Vercelli, A., 2011. Modulation of neuronal stem cell differentiation by hypoxia and reactive oxygen species. *Prog. Neurobiol.* 93, 444–455. <https://doi.org/10.1016/j.pneurobio.2011.01.007>.
- vom Saal, F.S., Nagel, S.C., Coe, B.L., Angle, B.M., Taylor, J.A., 2012. The estrogenic endocrine disrupting chemical bisphenol a (BPA) and obesity. *Mol. Cell. Endocrinol.* 354, 74–84. <https://doi.org/10.1016/j.mce.2012.01.001>.
- Williams, M.J., Akram, M., Barkauskaite, D., Patil, S., Kotsidou, E., Kheder, S., Vitale, G., Filafiero, M., Blemings, S.W., Maestri, G., Hazim, N., Vergoni, A.V., Schiöth, H.B., 2020. CCAP regulates feeding behavior via the NPf pathway in *Drosophila* adults. *Proc. Natl. Acad. Sci.* 117, 7401–7408. <https://doi.org/10.1073/pnas.1914037117>.
- Winget, S.W., Andrews, S., 2018. FastQ screen: a tool for multi-genome mapping and quality control. *F1000Res* 7, 1338. <https://doi.org/10.12688/f1000research.15931.2>.
- Wójtowicz, A.K., Sitarz-Głownia, A.M., Szczęśna, M., Szychowski, K.A., 2019. The action of Di-(2-Ethylhexyl) phthalate (DEHP) in mouse cerebral cells involves an impairment in aryl hydrocarbon receptor (AhR) signaling. *Neurotox. Res.* 35, 183–195. <https://doi.org/10.1007/s12640-018-9946-7>.
- Wójtowicz, A.K., Szychowski, K.A., Wnuk, A., Kajta, M., 2017. Dibutyl phthalate (DBP)-induced apoptosis and neurotoxicity are mediated via the aryl hydrocarbon receptor (AHR) but not by estrogen receptor alpha (ER $\alpha$ ), estrogen receptor Beta (ER $\beta$ ), or peroxisome proliferator-activated receptor gamma (PPAR $\gamma$ ) in mouse C. Neurotox. Res. 31, 77–89. <https://doi.org/10.1007/s12640-016-9665-x>.
- Yang, Q., Yang, X., Liu, J., Chen, Y., Shen, S., 2018. Effects of exposure to BPF on development and sexual differentiation during early life stages of zebrafish (*Danio rerio*). *Comp. Biochem. Physiol., Part C: Toxicol. Pharmacol.* 210, 44–56. <https://doi.org/10.1016/j.cbpc.2018.05.004>.

- Yuan, M., Chen, S., Zeng, C., Fan, Y., Ge, W., Chen, W., 2023. Estrogenic and non-estrogenic effects of bisphenol a and its action mechanism in the zebrafish model: an overview of the past two decades of work. *Environ. Int.* 176, 107976. <https://doi.org/10.1016/j.envint.2023.107976>.
- Zhang, X., Cheng, C., Zhang, G., Xiao, M., Li, L., Wu, S., Lu, X., 2021. Co-exposure to BPA and DEHP enhances susceptibility of mammary tumors via up-regulating Esr1/HDAC6 pathway in female rats. *Ecotoxicol. Environ. Saf.* 221, 112453. <https://doi.org/10.1016/j.ecoenv.2021.112453>.
- Zhang, X., Guo, N., Jin, H., Liu, R., Zhang, Z., Cheng, C., Fan, Z., Zhang, G., Xiao, M., Wu, S., Zhao, Y., Lu, X., 2022. Bisphenol a drives di(2-ethylhexyl) phthalate promoting thyroid tumorigenesis via regulating HDAC6/PTEN and c-MYC signaling. *J. Hazard. Mater.* 425, 127911. <https://doi.org/10.1016/j.jhazmat.2021.127911>.
- Zhang, Z.-N., Yang, D.-L., Liu, H., Bi, J., Bao, Y.-B., Ma, J.-Y., Zheng, Q.-X., Cui, D.-L., Chen, W., Xiang, P., 2023. Effects of TCPP and TCEP exposure on human corneal epithelial cells: oxidative damage, cell cycle arrest, and pyroptosis. *Chemosphere* 331, 138817. <https://doi.org/10.1016/j.chemosphere.2023.138817>.